Available online at www.sciencedirect.com

ScienceDirect

Nuclear Physics A 956 (2016) 280–283

NUCLEAR PHYSICS A

www.elsevier.com/locate/nuclphysa

The Rapidity Density Distributions and Longitudinal Expansion Dynamics of Identified Pions from the STAR Beam Energy Scan

Christopher E. Flores for the STAR Collaboration

University of California, Davis

Abstract

The Beam Energy Scan (BES) at the Relativistic Heavy-Ion Collider was proposed to characterize the properties of the medium produced in heavy-ion interactions over a broad range of baryon chemical potential. The aptitude of the STAR detector for mid-rapidity measurements has previously been leveraged to measure identified particle yields and spectra to extract bulk properties for the BES energies for $|y| \leq 0.1$. However, to extract information on expansion dynamics and full phase space particle production, it is necessary to study identified particle rapidity density distributions.
We present the first rapidity density distributions of identified pions from Au+Au collisions at $\sqrt{s_{NN}}$ = 7.7, 11.5, and 19.6 GeV from the BES program as measured by the STAR detector. We use these distributions to obtain the full phase space yields of the pions to provide additional information of the system's chemistry. Further, we report the width of the rapidity density distributions compared to the width expected from Landau hydrodynamics. Finally, we interpret the results as a function of collision energy and discuss them in the context of previous energy scans done at the AGS and SPS.

Keywords: Beam Energy Scan, STAR, pion, rapidity density distribution, full phase space yield, dale, transverse mass spectra

1. Introduction

Presently, a central effort of heavy-ion physics involves the exploration of the QCD phase diagram and the discovery of the structures which are expected to exist within it. Making progress in this effort is the driving purpose of the Beam Energy Scan (BES) Program at the Relativistic Heavy-Ion Collider (RHIC) which, since 2010, has varied the collision energy of Au+Au interactions. The result of varying the collision energy while keeping the colliding system the same is to change the medium's temperature, T, and baryon chemical potential, μ_B, thus probing various regions of the QCD phase space in search of signals corresponding to phase transition phenomena. [1]

Previous work in reference [2] regarding the characterization of T and μ_B has demonstrated the need for full phase space (4π) yields to accurately constrain these measures. In addition, previous work in references [3], [4], and [5] have posited that the softening of the equation of state (EOS) of the medium that is expected to coincide with a first order phase transition would manifest itself as a minimum in the speed of sound. Further, they suggest that such a minimum has been found in the ratio of the measured width of

http://dx.doi.org/10.1016/j.nuclphysa.2016.05.020

the rapidity density distribution of pions to the width expected by Landau hydrodynamics, σ_{hydro} ([6]), in results obtained from E895 ([7]), NA49 ([8]), and BRAHMS ([9]).

We address both the issue of characterizing the T and μ_B using full phase space yields and searching for first order phase transition phenomena associated with a change in the EOS by presenting the rapidity density distributions of identified π^- and π^+ mesons from the STAR BES program for the top 10% most central collisions of Au+Au ions at energies of $\sqrt{s_{NN}}$ = 19.6, 11.5, and 7.7 GeV. These distributions have been used to extract the full phase space yields which can be used to constrain the T and μ_B. Further, the width of these distributions give a measure of the longitudinal expansion of the resulting medium at the same energies and are used to investigate phase transition phenomena.

2. Analysis Details

The Solenoidal Tracker at RHIC (STAR) [10] is composed of several sub-detector systems and a magnet providing a half Tesla solenoidal field. For this analysis the two sub-detector systems of relevance are the Time Projection Chamber (TPC) [11] and the Time of Flight detector (TOF) [12]. The TPC is used for tracking particles within a broad momentum and η range and for particle idenitification via ionization energy loss measurements, $\frac{dE}{dx}$, for low momentum tracks, $m_T - m_0 < 0.5$ GeV/c^2. The TOF is used for particle identification for higher momentum tracks, $m_T - m_0 \geq 0.5$ GeV/c^2, via measurements of a track's velocity.

Tracks are reconstructed and associated with the vertex of a collision. Only events with z-vertex locations near the center of STAR ($|V_z| < 30$ cm) and with charged particle multiplicities consistent with top 10% central collisions are investigated in this analysis. Because the pion is the particle of interest, its mass is used to compute a value of rapidity, y, and transverse mass, $m_T - m_0$, for each track. These values are used to bin the tracks in rapidity (bin width = 0.1) and transverse mass (bin width = 0.025 GeV/c^2). Within each (y, $m_T - m_0$) bin the pion yield is extracted by fitting the $\frac{dE}{dx}$ or $\frac{1}{\beta}$ distributions with a sum of Gaussians (one for each particle species) and integrating the Gaussian of the pion.

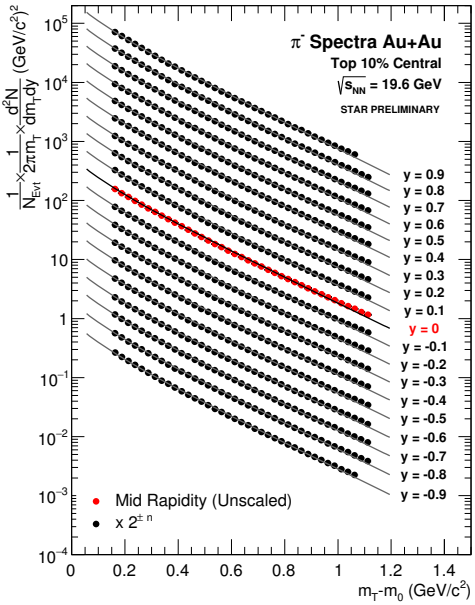

Fig. 1: The spectra of identified π^- mesons measured over two units of rapidity. The mid-rapidity spectrum is shown unscaled in red, while the spectra from forward (backward) rapidity bins are scaled up (down) by successive factors of 2 in black. Each spectrum is fit with a two-parameter Bose-Einstein function, which is integrated to obtain the $\frac{dN}{dy}$ for each rapidity bin.

The pion yields within each rapidity bin constitute a spectrum as a function of transverse mass. Each spectrum is corrected for detector efficiency and acceptance effects (the largest source of systematic uncertainty). As an example, the transverse mass spectra of π^- obtained from the $\sqrt{s_{NN}}$ = 19.6 GeV energy for all rapidity bins are shown in figure 1. These spectra are fit with a two parameter ($\frac{dN}{dy}$,T_{Slope}) Bose-Einstein function to obtain the $\frac{dN}{dy}$ for each rapidity bin. Since the Au+Au collision system is symmetric, the rapidity density distributions are symmeterized around $y_\pi = 0$ by means of a weighted average. The resulting rapidity density distributions for each of the three energies investigated are shown in figure 2.

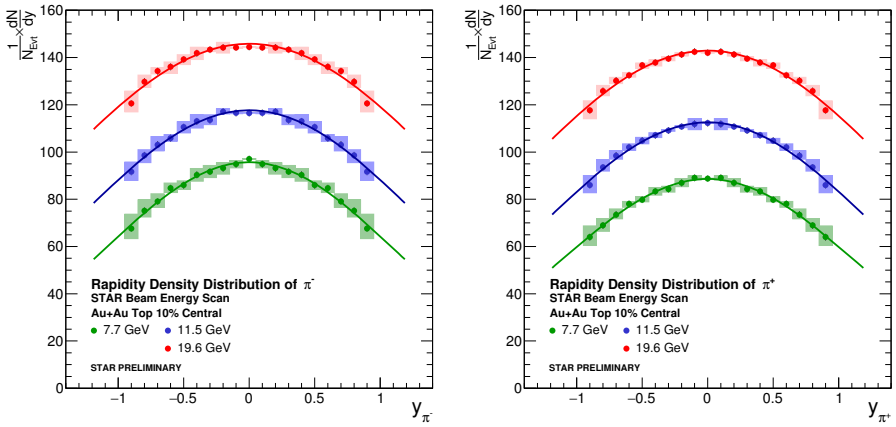

Fig. 2: The symmeterized rapidity density distributions for π^- (left) and π^+ (right) for top 10% central Au+Au collisions at $\sqrt{s_{NN}}$ = 7.7, 11.5, and 19.6 GeV. Each distribution is fit with a Gaussian function with a mean fixed at $y_\pi = 0$. Note that these distributions are not yet corrected for background or feed-down effects.

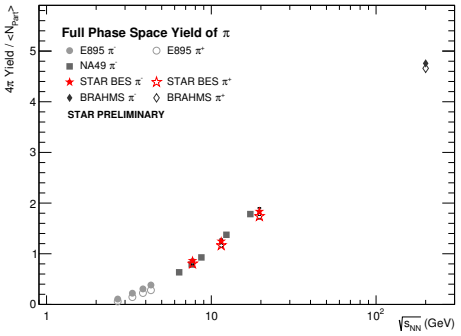

Fig. 3: The full phase space yield of π^+ and π^- obtained from the STAR BES program compared to results obtained from E895 [7], NA49 [8], and BRAHMS [9].

3. Results

The rapidity density distributions are each fit with a Gaussian function, per the Landau hydrodynamic model, with the mean fixed at $y_\pi = 0$. The fit functions are then used to obtain the full phase space yields and rapidity density widths at each energy. The resulting 4π yields and widths are shown in figures 3 and 4 (left), respectively, as a function of collision energy. For comparison the rapidity density distributions of π^-, and when possible π^+, from previous experiments were obtained from references [7], [8], and [9]. These distributions were refit with the same methodology described for the STAR data and the resulting 4π yields and widths are shown on the same figures.

As can be seen, the 4π yields from the STAR BES results are consistent with the trend established by previous experiments. It is also notable that the STAR BES results contribute 4π yield measuremets for both π^+ and π^- where previous results in this energy range from NA49 were for π^- only. Having both π^+ and π^- can aid in understanding effects sensitive to isospin. The measured width of the rapidity density distributions from the STAR BES data is also seen to reproduce the increasing trend as a function of collision energy reported by previous experiments.

Finally, the ratio of the measured width of π^- mesons, σ_π, to the expected width from Landau hydro-

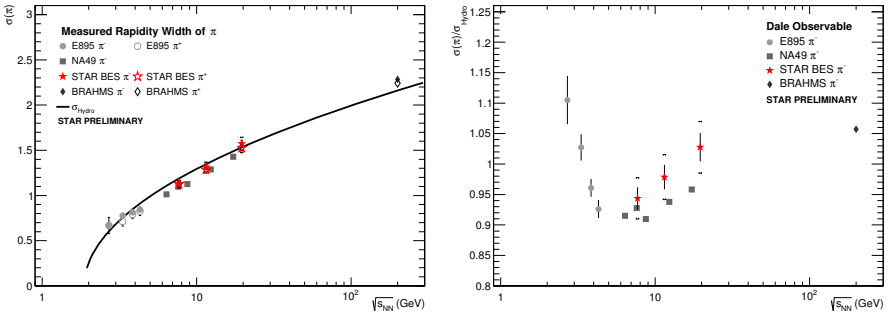

Fig. 4: Left: The measured widths of the π^+ and π^- rapidity density distributions and the expected width from Landau Hydrodynamics as a function of collision energy. Right: The "Dale" observable as a function of collision energy.

dynamics, σ_{hydro}, is computed to form the "Dale" observable and is shown in figure 4 (right). Again, for comparison, results obtained by refitting the data from previous experiments is shown as well. Here too we observe that the STAR BES results confirm the increasing trend from the previously observed minimum in the ratio over the measured energy range.

4. Conclusion

We have presented the first rapidity density distributions of identified particles from the STAR Beam Energy Scan program. Namely, we have extracted the rapidity density distributions of π^+ and π^- mesons from top 10% central Au+Au collisions at $\sqrt{s_{NN}} = 7.7$, 11.5, and 19.6 GeV. We have used these distributions to obtain the full phase space yields, rapidity density widths, and the ratio of the measured widths to the expected width from Landau hydrodynamics. The 4π yields and widths were seen to compare favorably to the results previously obtained by the NA49 experiment at similar energies and fit consistently into the over all trends observed as a function of collision energy from results reported by E895, NA49, and BRAHMS. Likewise, the "Dale" measurement obtained from the STAR BES results is seen to confirm the increasing trend in the measured energy range of the NA49 experiment.

5. Acknowledgements

This material is based upon work supported by the National Science Foundation under Grant No. 1404281. Any opinions, findings, and conclusions or recommendations expressed in this material are those of the authors and do not necessarily represent the views of the National Science Foundation.

References

[1] J. Cleymans, Physical Review C, 73, 034905 (2006).
[2] J. Cleymans, Journal of Physics G: Nuclear and Particle Physics, 37 094015 (2010).
[3] M. Bleicher, arXiv:hep-ph/0509314.
[4] H. Petersen and M. Bleicher, arXiv:nucl-th/0611001.
[5] A. Rustamov, Central European Journal of Physics, 10(6) 1267-1270 (2012).
[6] P. Carruthers and M. Duong-van, Physics Letters B 41, 597 (1972).
[7] J. L. Klay et al., Physics Review C 68, 05495 (2003).
[8] S. V. Afanasiev et al., Physics Review C 66, 054902 (2002).
[9] I.G. Bearden et al., Physics Review Letters 94, 162301 (2005).
[10] K. H. Ackermann et al., (STAR Collaboration), Nuclear Instruments and Methods in Physics Research Section A, 499 (2003) 624-632.
[11] M. Anderson, et al., Nuclear Instruments and Methods in Physics Research Section A, 499 (2003) 659.
[12] W.J. Llope et al., Nuclear Instruments and Methods in Physics Research Section A, 422 (2004) 252.